

Charmonium Decays of $Y(4260)$, $\psi(4160)$, and $\psi(4040)$

T. E. Coan,¹ Y. S. Gao,¹ F. Liu,¹ M. Artuso,² S. Blusk,² J. Butt,² J. Li,² N. Mena,² R. Mountain,² S. Nisar,² K. Randrianarivony,² R. Redjimi,² R. Sia,² T. Skwarnicki,² S. Stone,² J. C. Wang,² K. Zhang,² S. E. Csorna,³ G. Bonvicini,⁴ D. Cinabro,⁴ M. Dubrovin,⁴ A. Lincoln,⁴ D. M. Asner,⁵ K. W. Edwards,⁵ R. A. Briere,⁶ I. Brock,^{6,*} J. Chen,⁶ T. Ferguson,⁶ G. Tatishvili,⁶ H. Vogel,⁶ M. E. Watkins,⁶ J. L. Rosner,⁷ N. E. Adam,⁸ J. P. Alexander,⁸ K. Berkelman,⁸ D. G. Cassel,⁸ J. E. Duboscq,⁸ K. M. Ecklund,⁸ R. Ehrlich,⁸ L. Fields,⁸ R. S. Galik,⁸ L. Gibbons,⁸ R. Gray,⁸ S. W. Gray,⁸ D. L. Hartill,⁸ B. K. Heltsley,⁸ D. Hertz,⁸ C. D. Jones,⁸ J. Kandaswamy,⁸ D. L. Kreinick,⁸ V. E. Kuznetsov,⁸ H. Mahlke-Krüger,⁸ T. O. Meyer,⁸ P. U. E. Onyisi,⁸ J. R. Patterson,⁸ D. Peterson,⁸ E. A. Phillips,⁸ J. Pivarski,⁸ D. Riley,⁸ A. Ryd,⁸ A. J. Sadoff,⁸ H. Schwarthoff,⁸ X. Shi,⁸ S. Stroiney,⁸ W. M. Sun,⁸ T. Wilksen,⁸ M. Weinberger,⁸ S. B. Athar,⁹ P. Avery,⁹ L. Brevina-Newell,⁹ R. Patel,⁹ V. Potlia,⁹ H. Stoeck,⁹ J. Yelton,⁹ P. Rubin,¹⁰ C. Cawfield,¹¹ B. I. Eisenstein,¹¹ I. Karliner,¹¹ D. Kim,¹¹ N. Lowrey,¹¹ P. Naik,¹¹ C. Sedlack,¹¹ M. Selen,¹¹ E. J. White,¹¹ J. Wiss,¹¹ M. R. Shepherd,¹² D. Besson,¹³ T. K. Pedlar,¹⁴ D. Cronin-Hennessy,¹⁵ K. Y. Gao,¹⁵ D. T. Gong,¹⁵ J. Hietala,¹⁵ Y. Kubota,¹⁵ T. Klein,¹⁵ B. W. Lang,¹⁵ R. Poling,¹⁵ A. W. Scott,¹⁵ A. Smith,¹⁵ S. Dobbs,¹⁶ Z. Metreveli,¹⁶ K. K. Seth,¹⁶ A. Tomaradze,¹⁶ P. Zweber,¹⁶ J. Ernst,¹⁷ H. Severini,¹⁸ S. A. Dytman,¹⁹ W. Love,¹⁹ V. Savinov,¹⁹ O. Aquines,²⁰ Z. Li,²⁰ A. Lopez,²⁰ S. Mehrabyan,²⁰ H. Mendez,²⁰ J. Ramirez,²⁰ G. S. Huang,²¹ D. H. Miller,²¹ V. Pavlunin,²¹ B. Sanghi,²¹ I. P. J. Shipsey,²¹ B. Xin,²¹ G. S. Adams,²² M. Anderson,²² J. P. Cummings,²² I. Danko,²² J. Napolitano,²² Q. He,²³ J. Insler,²³ H. Muramatsu,²³ C. S. Park,²³ and E. H. Thorndike²³

(CLEO Collaboration)

¹*Southern Methodist University, Dallas, Texas 75275*

²*Syracuse University, Syracuse, New York 13244*

³*Vanderbilt University, Nashville, Tennessee 37235*

⁴*Wayne State University, Detroit, Michigan 48202*

⁵*Carleton University, Ottawa, Ontario, Canada K1S 5B6*

⁶*Carnegie Mellon University, Pittsburgh, Pennsylvania 15213*

⁷*Enrico Fermi Institute, University of Chicago, Chicago, Illinois 60637*

⁸*Cornell University, Ithaca, New York 14853*

⁹*University of Florida, Gainesville, Florida 32611*

¹⁰*George Mason University, Fairfax, Virginia 22030*

¹¹*University of Illinois, Urbana-Champaign, Illinois 61801*

¹²*Indiana University, Bloomington, Indiana 47405*

¹³*University of Kansas, Lawrence, Kansas 66045*

¹⁴*Luther College, Decorah, Iowa 52101*

¹⁵*University of Minnesota, Minneapolis, Minnesota 55455*

¹⁶*Northwestern University, Evanston, Illinois 60208*

¹⁷*State University of New York at Albany, Albany, New York 12222*

¹⁸*University of Oklahoma, Norman, Oklahoma 73019*

¹⁹*University of Pittsburgh, Pittsburgh, Pennsylvania 15260*

²⁰*University of Puerto Rico, Mayaguez, Puerto Rico 00681*

²¹*Purdue University, West Lafayette, Indiana 47907*
²²*Rensselaer Polytechnic Institute, Troy, New York 12180*
²³*University of Rochester, Rochester, New York 14627*

(Dated: February 20, 2006)

Abstract

Using data collected with the CLEO detector operating at the CESR e^+e^- collider at $\sqrt{s} = 3.97$ - 4.26 GeV, we investigate 15 charmonium decay modes of the $\psi(4040)$, $\psi(4160)$, and $Y(4260)$ resonances. We confirm, at 11σ significance, the BABAR $Y(4260) \rightarrow \pi^+\pi^-J/\psi$ discovery, make the first observation of $Y(4260) \rightarrow \pi^0\pi^0J/\psi$ (5.1σ), and find the first evidence for $Y(4260) \rightarrow K^+K^-J/\psi$ (3.7σ). We measure e^+e^- cross-sections at $\sqrt{s} = 4.26$ GeV as $\sigma(\pi^+\pi^-J/\psi) = 58_{-10}^{+12} \pm 4$ pb, $\sigma(\pi^0\pi^0J/\psi) = 23_{-8}^{+12} \pm 1$ pb, and $\sigma(K^+K^-J/\psi) = 9_{-5}^{+9} \pm 1$ pb, in which the uncertainties are statistical and systematic, respectively. Upper limits are placed on other decay rates from all three resonances.

*Current address: Universität Bonn, Nussallee 12, D-53115 Bonn

The region at center-of-mass energies above charmonium open-flavor production threshold is of great interest to theory due to its richness of $c\bar{c}$ states, the properties of which are not well-understood. Prominent structures in the hadronic cross-section are the $\psi(3770)$, the $\psi(4040)$, and the $\psi(4160)$ [1]. Their main characteristics are large total widths, two orders of magnitude larger than for the lower-lying $c\bar{c}$ states of $J^{PC} = 1^{--}$, and weaker couplings to leptons than the J/ψ and $\psi(2S)$. Decays to closed-charm final states are not favored due to the availability of open-charm channels.

Recently, observations of new charmonium-like states in the same energy region have been reported [2]. Most of these have been observed to decay through open charm. However, an enhancement in the invariant mass spectrum of the closed-charm $\pi^+\pi^-J/\psi$ final state has also been observed by BABAR in initial state radiation (ISR), $e^+e^- \rightarrow \gamma(\pi^+\pi^-J/\psi)$ [3]. A weaker signal was observed in the decay $B \rightarrow K(\pi^+\pi^-J/\psi)$ [4]. The observed lineshape can be described by a single resonance, termed $Y(4260)$, of mass $M = 4259 \pm 8_{-6}^{+2}$ MeV, width $\Gamma_{\text{tot}} = 88 \pm 23_{-4}^{+6}$ MeV, and coupling $\Gamma_{ee} \times \mathcal{B}(Y(4260) \rightarrow \pi^+\pi^-J/\psi) = 5.5 \pm 1.0_{-0.7}^{+0.8}$ eV. It is located quite unexpectedly at a local *minimum* of the hadronic cross-section. Since it is observed in ISR, the new state must have $J^{PC} = 1^{--}$, and therefore it can be studied directly in e^+e^- collisions at threshold. No other evidence for a resonance at this mass has been identified [5], leaving the existence and possible charmonium-like nature of this state uncertain. Many interpretations have been suggested; to be compatible with the absence of a corresponding enhancement in open charm production, most favor an unconventional explanation of $Y(4260)$, such as hybrid charmonium [6, 7], tetraquarks [8–10], or hadronic molecules [11–13]. One proposal [14] argues that $Y(4260)$ is conventional: It identifies $Y(4260)$ with the $\psi(4S)$ vector $c\bar{c}$ state, and relies upon interference effects to produce the dip in open-charm cross-section and a hypothesized large coupling to $\pi^+\pi^-J/\psi$ of the $\psi(3S)$, commonly associated with the $\psi(4040)$.

To further clarify the nature of $Y(4260)$, investigation of both open and closed charm is necessary. Here, we report production cross-sections measurements of 16 final states containing a J/ψ , $\psi(2S)$, χ_{cJ} , or ϕ , in the $\psi(4040)$, $\psi(4160)$, and $Y(4260)$ energy region, motivated by the range of experimental tests suggested so far [6–14]. We use data taken during a scan of center-of-mass energies $\sqrt{s} = 3.97\text{--}4.26$ GeV, complementing a sample of an integrated luminosity $\int \mathcal{L} dt = 281 \text{ pb}^{-1}$ at $\sqrt{s} = 3.773$ GeV previously acquired. Collisions were registered with the CLEO detector [15] at the CESR e^+e^- collider [16]. The scan data naturally separate into three regions: the $\psi(4040)$ ($\sqrt{s} = 3.97\text{--}4.06$ GeV, $\int \mathcal{L} dt = 20.7 \text{ pb}^{-1}$), the $\psi(4160)$ (4.12–4.20 GeV, 26.3 pb^{-1}), and $\sqrt{s} = 4.26$ GeV (13.2 pb^{-1}). Fig. 1(a) shows a profile of $\int \mathcal{L} dt$ vs. \sqrt{s} and Fig. 1(b) the Born-level Breit-Wigner lineshapes [1] for the four resonances between $\sqrt{s}=3.7$ and 4.4 GeV, also indicating the grouping of scan points. We estimate the number of resonances produced by folding together the luminosities with the resonance Breit-Wigner cross-sections [17], including radiative corrections [18, 19], and arrive at $(93 \pm 11) \times 10^3$ [$(115 \pm 15) \times 10^3$] $\psi(4040)$ [$\psi(4160)$] mesons, where the dominant errors are the uncertainties on resonance parameters.

The CLEO detector [15] features a solid angle coverage of 93% for charged and neutral particles. The charged particle tracking system operates in a 1.0 T magnetic field parallel to the beam axis and achieves a momentum resolution of $\sim 0.6\%$ at momenta of 1 GeV/ c . The CsI crystal calorimeter attains photon energy resolutions of 2.2% for $E_\gamma=1$ GeV and 5% at 100 MeV. Particle identification is performed with the specific ionization loss (dE/dx) and the Ring Imaging Cherenkov detector (RICH). Muons of momentum $p > 1$ GeV are separated from pions by their penetration of the calorimeter, solenoid coil, and up to three

36-cm-thick slabs of magnet iron for subsequent detection by wire chambers behind each slab. The integrated luminosity was measured using e^+e^- , $\gamma\gamma$, and $\mu^+\mu^-$ events [20, 21].

The final states analyzed here are listed in Table I. We require all particles in each final state to be reconstructed, and four-momentum conservation is enforced. Mass windows for the following light hadron decays are set, based on MC studies: $\pi^0 \rightarrow \gamma\gamma$ (110-150 MeV); $\eta \rightarrow \gamma\gamma$, $\eta \rightarrow \pi^+\pi^-\pi^0$ (450-650 MeV); $\eta' \rightarrow \pi^+\pi^-\eta$, $\eta' \rightarrow \gamma\pi^+\pi^-$ (930-980 MeV); $\omega \rightarrow \pi^+\pi^-\pi^0$ (730-830 MeV); and $\phi \rightarrow K^+K^-$ (1.00-1.04 GeV).

We identify a J/ψ or $\psi(2S)$ through its decay into $\ell^+\ell^-$, $\ell^+\ell^-=e^+e^-$ or $\mu^+\mu^-$. A lepton candidate is identified by the ratio of the energy deposited in the calorimeter, E , to the measured momentum, p . Muon pair candidates must satisfy $E/p < 0.25$ for at least one of the tracks and $E/p < 0.5$ for the other; both electrons must have $E/p > 0.85$ and a dE/dx consistent with the value expected for an electron. Pions faking muons are additionally suppressed by requiring at least one muon candidate per muon pair to leave a signature in the muon system. A lepton pair is classified as a J/ψ [$\psi(2S)$] $\rightarrow \ell^+\ell^-$ candidate if the invariant mass of the decay products lies within 3.04-3.14 [3.64-3.73] GeV. We also use the decay $\psi(2S) \rightarrow \pi^+\pi^-J/\psi$, where we require $M(\pi^+\pi^-J/\psi) = 3.64-3.73$ GeV.

A $\gamma\chi_{c1,2} \rightarrow \gamma\gamma J/\psi$ decay is tagged by the highest energy photon in the event having an energy within $(-60, +40)$ MeV of $E_\gamma = (s - M_{\chi_{cJ}}^2)/2\sqrt{s}$. Events with $M(\gamma\gamma)$ in the π^0 or η mass ranges are excluded. Any calorimeter shower other than the two radiative transition photon candidates must have $E < 50$ MeV. We select $\pi^+\pi^-\pi^0\chi_{cJ}$, $\chi_{cJ} \rightarrow \gamma J/\psi$ events ($J = 1, 2$) by demanding that $M(\gamma J/\psi)$ as well as the mass recoiling against the $\pi^+\pi^-\pi^0$ match $M_{\chi_{cJ}}$ [1] within ± 20 MeV.

For K^+K^-J/ψ , the kaons have momenta that are too low for use of the RICH detector, so π^\pm rejection is achieved by requiring that at least one of the K^\pm candidates have momentum in the range 0.2-0.5 GeV/ c and have dE/dx within three standard deviations of the expected value for a K^\pm . For $\pi^+\pi^-\phi$ and $\chi_{c0} \rightarrow 2(\pi^+\pi^-)$ or $\pi^+\pi^-K^+K^-$, K^\pm candidates must be positively identified as a kaon using a likelihood based upon both dE/dx and RICH responses, but none of the π^\pm candidates in either decay can be so identified as kaons. For the $\omega\chi_{c0}$ mode, both the mass of the χ_{c0} decay products and the mass recoiling against the ω must lie within 50 MeV of $M(\chi_{c0})$ [1]. Similarly, for $\pi^+\pi^-\phi$, the mass recoiling against $\pi^+\pi^-$ must lie in the range 0.94-1.10 GeV.

For $\pi^+\pi^-J/\psi$ and $\pi^+\pi^-\psi(2S)$, we require that $M(\pi^+\pi^-) > 350$ MeV and that neither pion candidate be identified as an electron via E/p and dE/dx as above. These cuts suppress $e^+e^- \rightarrow \ell^+\ell^-\gamma$, $\gamma \rightarrow e^+e^-$ events in which the e^+e^- pair from the photon conversion is mistaken for the $\pi^+\pi^-$. For π^0J/ψ as well as the $\eta J/\psi$ and $\gamma\chi_{c1,2}$ modes that end in $\gamma\gamma e^+e^-$, background from Bhabha events is diminished by requiring $\cos\theta_{e^+} < 0.3$.

For modes with a J/ψ or $\psi(2S)$ we restrict the missing momentum k , computed from the measured event momenta according to Eq. (6) of Ref. [22], to further reduce background. Signal events will have $k \approx 0$; selection windows are set separately for each mode according to the measurement resolution predicted by MC simulation, and range from ± 10 MeV (K^+K^-J/ψ) and ± 15 MeV ($\pi^+\pi^-J/\psi$) to $(-35, +75)$ MeV ($\pi^0\pi^0J/\psi$).

Backgrounds in the XJ/ψ modes from $e^+e^- \rightarrow \gamma^* \rightarrow$ hadrons are estimated from the yields seen in the data with the restrictions on $M(\ell^+\ell^-)$ and k adjusted to correspond to masses either below or above $M_{J/\psi}$. The sideband windows, $|k| < 150$ MeV and either $M(\ell^+\ell^-) = 2.90 \pm 0.15$ GeV or 3.30 ± 0.15 GeV, are considerably wider than the signal regions, allowing for the accumulation of more statistics in the background estimates, and therefore are scaled down by the sideband/signal window width ratios prior to subtrac-

tion from the signal yields. The sideband scale factors are verified in MC simulations of $e^+e^- \rightarrow \gamma^* \rightarrow \text{hadrons}$. We perform a mass sideband subtraction for the χ_{c0} , as a result of which all observed events can be attributed to background, and for ϕ and η' , also reducing the yield substantially; photon energy sidebands are used to estimate background in $\gamma\chi_{cJ}$. Background in $\pi\pi J/\psi$, $\eta J/\psi$, and $\gamma\chi_{cJ}$ modes produced in $\gamma\psi(2S)$ decay (with $M(\psi(2S)) \approx \sqrt{s} \gg 3686 \text{ MeV}$) is summed along with that from the sidebands in Table I, and comprises 10-40% of the total background in those modes. Other modes could be subjected to similar subtractions, but due to the absence of significant event populations, we forgo this option, and use uncorrected yields to compute (conservative) upper limits.

The EVTGEN event generator [24], which includes final state radiation [23], and a GEANT-based [25] detector simulation are used to model the physics processes. The generator implements a relative S -wave (P -wave) configuration between the $\pi\pi$ (η or π^0) and the J/ψ or $\psi(2S)$. Detection efficiencies (Table I) range from 4-38%, not including the effects of the intermediate branching fractions [1, 26] for $J/\psi \rightarrow \ell^+\ell^-$, $\psi(2S) \rightarrow \ell^+\ell^-$, $\psi(2S) \rightarrow \pi^+\pi^- J/\psi$, $\chi_{cJ} \rightarrow \gamma J/\psi$, or $\chi_{c0} \rightarrow \text{hadrons}$, but including those for π^0 , η , ω , η' , and ϕ decay. Already included are the effects of ISR, which reduce efficiencies by relative fractions of 8-21%.

The radiative return process $e^+e^- \rightarrow \gamma\psi(2S) \rightarrow XJ/\psi$ results in final states which are nearly identical to some of our signal modes, and thereby affords an opportunity to verify our understanding of efficiencies, background, and luminosity. To gather such events, we alter only the k -windows of the event selections, as such events will congregate not near $k = 0$ but rather around $k_0 = (s - M_{\psi(2S)}^2)/2\sqrt{s}$. The cross-section for this process can be calculated by integrating the convolution of a Breit-Wigner lineshape (approximated by a δ -function) with the ISR kernel W from Eq. (28) of Ref. [18]:

$$\sigma(e^+e^- \rightarrow \gamma\psi(2S)) = \frac{12\pi^2\Gamma_{ee}}{sM_{\psi(2S)}} \times W(s, 2k_0/\sqrt{s}). \quad (1)$$

This curve as well as the cross-section measurements using $\psi(2S) \rightarrow XJ/\psi$, $X=\pi^+\pi^-$, $\pi^0\pi^0$, and η [26], are shown in Figure 1(c). The CLEO value for $\Gamma_{ee}[\psi(2S)]$ [22] sets the scale of the theoretical curve in the figure. The predicted number of observed radiative return events for the three channels together in all the scan data is 820 ± 21 , which compares favorably to 825 ± 29 events seen.

Table I lists cross-section results for the $k = 0$ region. Cross-section central values and errors are shown when the statistical significance (the likelihood that the observed event yield is due entirely to background) exceeds 2.5σ ; otherwise upper limits at 90% confidence level (CL) are shown. Poisson fluctuations of the background are taken into account in the computation of statistical uncertainties. Cross-sections for $e^+e^- \rightarrow \pi\pi J/\psi$ vs. \sqrt{s} are shown in Fig. 1(d); selected missing momentum and dipion mass distributions appear in Figs. 2 and 3, respectively. The yields for $\pi^+\pi^-\phi$ are consistent with the rate observed [27] from $e^+e^- \rightarrow \gamma^*$ at $\sqrt{s}=3.67 \text{ GeV}$.

Systematic uncertainties arise from the following sources: luminosity (2%), charged particle tracking (1% per track), particle identification (1% per high momentum e , π , or K ; 5% per K in K^+K^-J/ψ), 3% per μ pair for muon chamber modeling, and a mode-dependent contribution amounting to 50% of the total estimated background. Statistical uncertainties dominate. The total systematic error excluding the background uncertainty amounts to approximately 10% for most channels (up to 30% for χ_{cJ} modes and $\pi^+\pi^-\phi$). The only charmonium channels with more than 2.5σ statistical significance are, at $\sqrt{s}=4.260 \text{ GeV}$, $\pi^+\pi^- J/\psi$

(11σ), $\pi^0\pi^0 J/\psi$ (5.1σ), and $K^+K^- J/\psi$ (3.7σ); in the $\psi(4160)$ dataset, $\pi^+\pi^- J/\psi$ (3.6σ) and $\pi^0\pi^0 J/\psi$ (2.6σ); and in the $\psi(4040)$ dataset, $\pi^+\pi^- J/\psi$ (3.3σ). The $\psi(4160)$ -region yields of $\pi^+\pi^- J/\psi$ and $\pi^0\pi^0 J/\psi$ are consistent with being due entirely to the $Y(4260)$ low-side tail [3]. No compelling evidence is found for any other decays in the three resonance regions, and corresponding upper limits on cross-sections (and, for $\psi(4040)$ and $\psi(4160)$ datasets, on branching fractions) are set. In particular, we find $\mathcal{B}(\psi(4040) \rightarrow \pi^+\pi^- J/\psi) < 0.4\%$ and $\mathcal{B}(\psi(4160) \rightarrow \pi^+\pi^- J/\psi) < 0.4\%$. These correspond to partial widths of less than 0.4 MeV in both cases, to be compared with the central values for $\psi(2S)$ and $\psi(3770)$ of 0.10 MeV and 0.44 MeV [1], respectively. While statistics are low, no prominent narrow features emerge in $M(\pi^+\pi^-)$, and the distribution is somewhat softer than the $\psi(2S)$ -like MC prediction.

This analysis provides a high-significance confirmation of the BABAR signal of $\pi^+\pi^- J/\psi$. The observation of the $\pi^0\pi^0 J/\psi$ mode disfavors the $\chi_{cJ}\rho^0$ molecular model [11]. The fact that the $\pi^0\pi^0 J/\psi$ rate is about half that of $\pi^+\pi^- J/\psi$ disagrees with the prediction of the baryonium model [12]. Our evidence of significant $K^+K^- J/\psi$ production is not compatible with these two models either. No evidence of a large $\pi^+\pi^- J/\psi$ signal from the $\psi(4040)$ is observed, making the conventional $Y(4260)=\psi(4S)$ assignment [14] less attractive. The results are compatible with hybrid charmonium interpretations [6, 7], but open-charm studies will be required to make more definitive conclusions. A large coupling to $D_1(2430)^0\bar{D}_0$ and a small one to $D_s\bar{D}_s$ signals hybrid charmonium [6], whereas a dominant $D_s\bar{D}_s$ ($D\bar{D}$) could favor a $c\bar{s}s\bar{c}$ [6, 9] ($c\bar{q}q\bar{c}$ [8]) tetraquark model.

We gratefully acknowledge the effort of the CESR staff in providing us with excellent luminosity and running conditions. This work was supported by the A.P. Sloan Foundation, the National Science Foundation, and the U.S. Department of Energy.

-
- [1] S. Eidelman *et al.* (Particle Data Group), Phys. Lett. B **592**, 1 (2004), and 2005 partial update for edition 2006.
 - [2] E.J. Eichten, K. Lane, and C. Quigg, Phys. Rev. D **73**, 014014 (2006); E. Swanson, hep-ph/0601110 (2006).
 - [3] B. Aubert *et al.* (BABAR Collaboration), Phys. Rev. Lett. **95**, 142001 (2005) [arXiv:hep-ex/0506081].
 - [4] B. Aubert *et al.* (BABAR Collaboration), Phys. Rev. D **73**, 011101(R) (2006)[arXiv:hep-ex/0507090].
 - [5] B. Aubert *et al.* (BABAR Collaboration), arXiv:hep-ex/0512023 (2005).
 - [6] F.E. Close and P.R. Page, Phys. Lett. B **628**, 215 (2005).
 - [7] S.-L. Zhu, Phys. Lett. B **625**, 212 (2005); E. Kou and O. Pene, Phys. Lett. B **631**, 164 (2005); X.L. Luo and Y. Liu, hep-lat/0512044 (2005).
 - [8] D. Ebert, R.N. Faustov, and V.O. Galkin, hep-ph/0512230 (2005) (accepted by Phys. Lett. B).
 - [9] L. Maiani *et al.*, Phys. Rev. D **72**, 031502 (2005),
 - [10] T.-W. Chiu and T.H. Hsieh (TWQCD Collaboration), hep-lat/0512029 (2005).
 - [11] X. Liu, X.-Q. Zeng, and X.-Q. Li, Phys. Rev. D **72**, 054023 (2005).
 - [12] C.-F. Qiao, hep-ph/0510228 (2005).
 - [13] C.Z. Yuan, P. Wang, and X.H. Mo, hep-ph/0511107 (2005).
 - [14] F.J. Llanes-Estrada, Phys. Rev. D **72**, 031503 (2005).

- [15] Y. Kubota *et al.* (CLEO Collaboration), Nucl. Instrum. Meth. A **320**, 66 (1992); M. Artuso *et al.*, Nucl. Instrum. Meth. A **554**, 147 (2005) [arXiv:physics/0506132]; D. Peterson *et al.*, Nucl. Instrum. Meth. A **478**, 142 (2002).
- [16] R.A. Briere *et al.* (CLEO-c/CESR-c Taskforces, CLEO-c Collaboration), Cornell LEPP preprint CLNS 01/1742 (2001), unpublished.
- [17] K. K. Seth, Phys. Rev. D **72**, 017501 (2005).
- [18] E.A. Kuraev and V.S. Fadin, Sov. J. Nucl. Phys. **41**, 466 (1985).
- [19] G. Bonneau and F. Martin, Nucl. Phys. **B27**, 381 (1971); J.P. Alexander *et al.*, Nucl. Phys. **B320**, 45 (1989).
- [20] G. Crawford *et al.* (CLEO Collaboration), Nucl. Instrum. Methods Phys. Res., Sect. A **345**, 429 (1992).
- [21] C.M. Carloni Calame *et al.*, Nucl. Phys. Proc. Suppl. B **131**, 48 (2004).
- [22] N. E. Adam *et al.* (CLEO Collaboration), arXiv:hep-ex/0508023 (accepted by Phys. Rev. Lett.).
- [23] E. Barberio and Z. Was, Comput. Phys. Commun. **79**, 291 (1994).
- [24] D.J. Lange, Nucl. Instrum. Methods Phys. Res., Sect. A **462**, 152 (2001).
- [25] R. Brun *et al.*, Geant 3.21, CERN Program Library Long Writeup W5013 (1993), unpublished.
- [26] N.E. Adam *et al.* (CLEO Collaboration), Phys. Rev. Lett. **94**, 232002 (2005).
- [27] R.A. Briere *et al.* (CLEO Collaboration), Phys. Rev. Lett. **95**, 062001 (2005).

TABLE I: For each mode $e^+e^- \rightarrow X$, for three center-of-mass regions: the detection efficiency, ϵ ; the number of signal [background] events in data, N_s [N_b]; the cross-section $\sigma(e^+e^- \rightarrow X)$; and the branching fraction of $\psi(4040)$ or $\psi(4160)$ to X , \mathcal{B} . Upper limits are at 90% CL. ‘-’ indicates that the channel is kinematically or experimentally inaccessible.

Channel	$\sqrt{s} = 3970 - 4060$ MeV					$\sqrt{s} = 4120 - 4200$ MeV					$\sqrt{s} = 4260$ MeV			
	ϵ (%)	N_s	N_b	σ (pb)	\mathcal{B} (10^{-3})	ϵ (%)	N_s	N_b	σ (pb)	\mathcal{B} (10^{-3})	ϵ (%)	N_s	N_b	σ (pb)
$\pi^+\pi^-J/\psi$	37	12	3.7	$9_{-4}^{+5} \pm 2$	< 4	38	13	3.7	$8_{-3}^{+4} \pm 2$	< 4	38	37	2.4	$58_{-10}^{+12} \pm 4$
$\pi^0\pi^0J/\psi$	20	1	1.9	< 8	< 2	21	5	0.9	$6_{-3}^{+5} \pm 1$	< 3	22	8	0.3	$23_{-8}^{+12} \pm 1$
K^+K^-J/ψ				-		7	1	0.07	< 20	< 5	21	3	0.07	$9_{-5}^{+9} \pm 1$
$\eta J/\psi$	19	12	9.5	< 29	< 7	16	15	8.8	< 34	< 8	16	5	2.7	< 32
$\pi^0 J/\psi$	23	2		< 10	< 2	22	1		< 6	< 1	22	1		< 12
$\eta' J/\psi$				-		11	4	2.5	< 23	< 5	11	0	1.5	< 19
$\pi^+\pi^-\pi^0 J/\psi$	21	1		< 8	< 2	21	0		< 4	< 1	22	0		< 7
$\eta\eta J/\psi$				-					-		6	1		< 44
$\pi^+\pi^-\psi(2S)$				-		12	0		< 15	< 4	19	0		< 20
$\eta\psi(2S)$				-					-		15	0		< 25
$\omega\chi_{c0}$				-					-		9	11	11.5	< 234
$\gamma\chi_{c1}$	26	9	8.1	< 50	< 11	26	11	8.7	< 45	< 10	26	1	3.3	< 30
$\gamma\chi_{c2}$	25	6	8.0	< 76	< 17	26	10	8.6	< 79	< 18	27	4	3.3	< 90
$\pi^+\pi^-\pi^0\chi_{c1}$	6	0		< 47	< 11	8	0		< 26	< 6	9	0		< 46
$\pi^+\pi^-\pi^0\chi_{c2}$	4	0		< 141	< 32	8	0		< 56	< 13	9	0		< 96
$\pi^+\pi^-\phi$	17	26	3.0	< 12	< 3	17	17	6.0	< 5	< 1	18	7	5.5	< 5

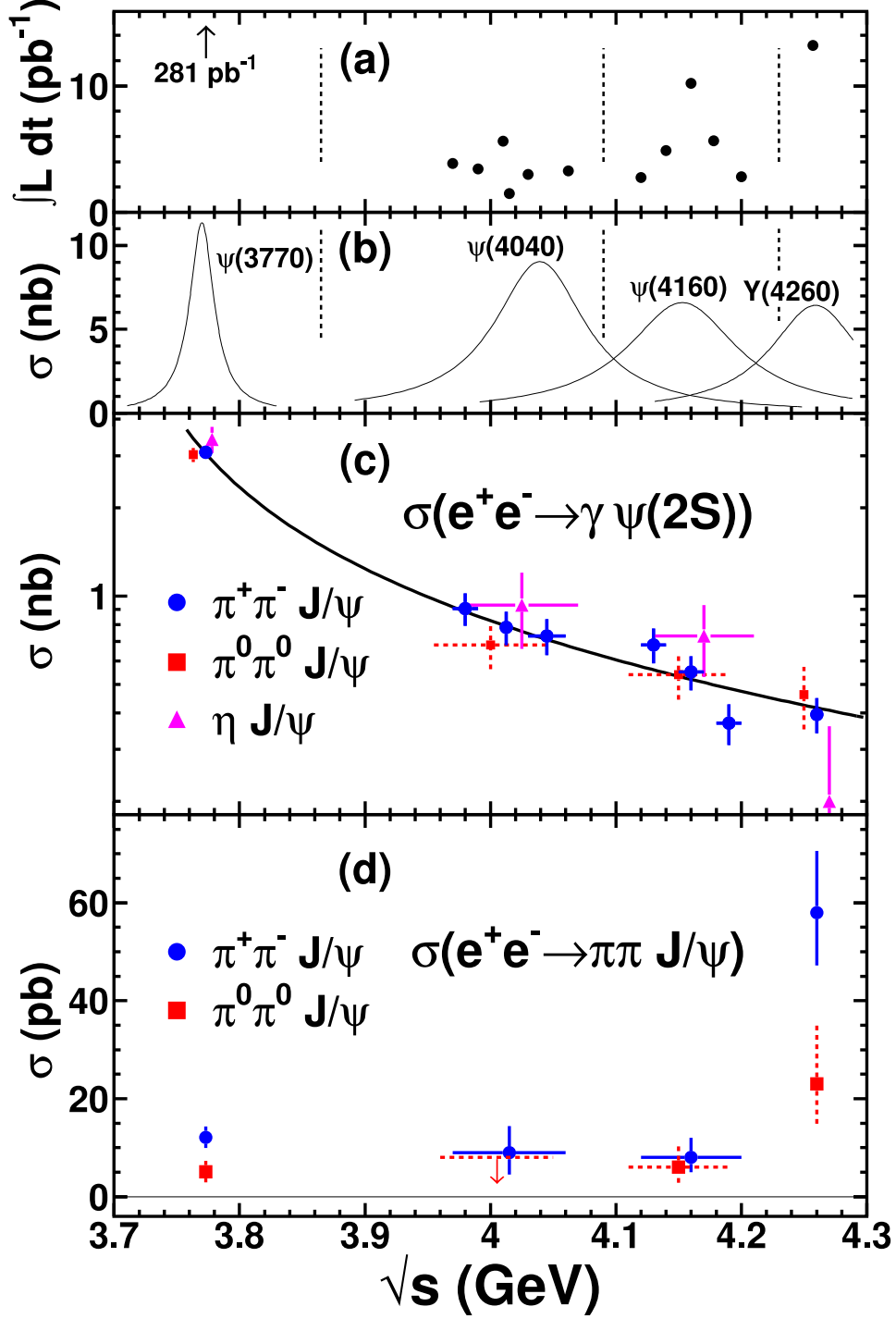


FIG. 1: (a) $\int \mathcal{L} dt$ vs. \sqrt{s} (circles). (b) Born-level Breit-Wigner cross-sections for resonances in this energy region; the $Y(4260)$ curve has an arbitrary vertical scale. (c) $e^+e^- \rightarrow \gamma\psi(2S)$ cross-section measurements vs. \sqrt{s} from $\pi^+\pi^-J/\psi$ (circles), $\pi^0\pi^0J/\psi$ (squares, dashed lines), and $\eta J/\psi$ (triangles) overlaid with the theoretical prediction as described in the text. (d) Cross-sections for $e^+e^- \rightarrow \pi^+\pi^-J/\psi$ (circles) and $\pi^0\pi^0J/\psi$ (squares, dashed lines) vs. \sqrt{s} . Some points in (c) and (d) are offset in \sqrt{s} by 10 MeV for display purposes.

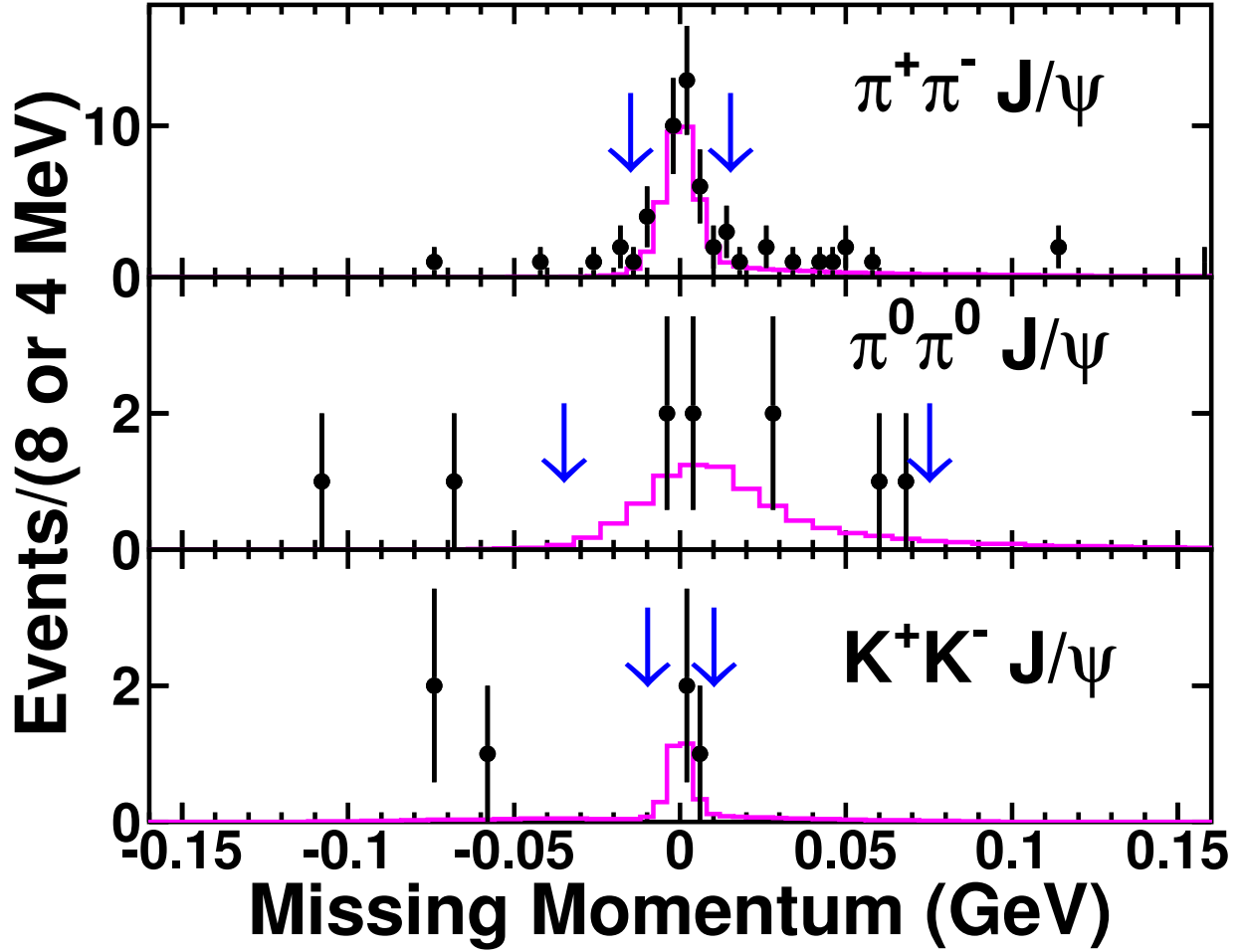


FIG. 2: The missing momentum (k) distribution for $\pi^+\pi^-J/\psi$ (top), $\pi^0\pi^0J/\psi$ (middle), and K^+K^-J/ψ (bottom) in the data at $\sqrt{s} = 4.26$ GeV (circles), and the signal shape as predicted by MC simulation (solid line histogram) scaled to the net signal size.

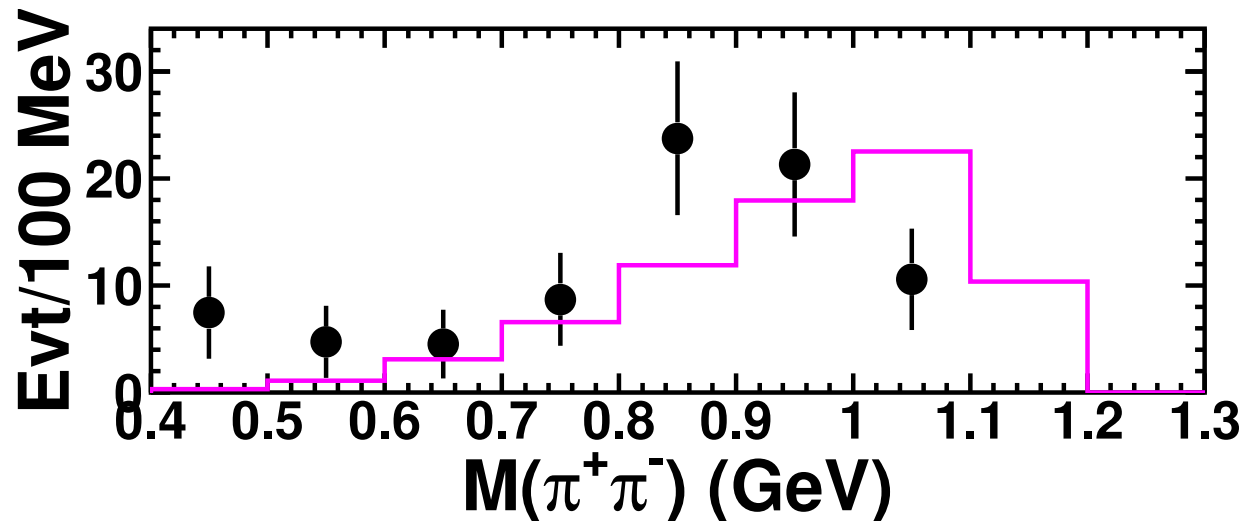


FIG. 3: The efficiency-corrected dipion invariant mass distribution for the $\pi^+\pi^-J/\psi$ final state in the signal region at $\sqrt{s} = 4.26$ GeV for the data (circles) and the signal shape (solid line histogram) as predicted by $\psi(2S)$ -like MC simulation scaled to the net signal size.